Molecular Pharmacology Fast Forward. Published on April 22, 2010 as doi:10.1124/mol.110.064345
This article has not been copyedited and formatted. The final version may differ from this version.

MOL # 64345

Title Page

Orthosteric and allosteric modes of interaction of novel selective agonists of the M_1 muscarinic acetylcholine receptor

Vimesh A. Avlani, Christopher J. Langmead, Elizabeth Guida, Martyn D. Wood, Ben G. Tehan, Hugh J. Herdon, Jeannette M. Watson, Patrick M. Sexton and Arthur Christopoulos

Drug Discovery Biology, Monash Institute of Pharmaceutical Sciences and Department of Pharmacology, Monash University, Melbourne, Australia (VAA, EG, PMS, AC) and GlaxoSmithKline, Harlow, Essex, UK (MDW, CJL, JW, BGT, HJH, JMW).

Running title: Characterization of novel selective muscarinic agonists

Molecular Pharmacology Fast Forward. Published on April 22, 2010 as DOI: 10.1124/mol.110.064345
This article has not been copyedited and formatted. The final version may differ from this version.

MOL # 64345

Running title page

Running title (60 characters): Characterization of novel selective muscarinic agonists

Corresponding author: Prof Arthur Christopoulos
Drug Discovery Biology and
Department of Pharmacology
Monash Institute of Pharmaceutical Sciences
Monash University
Parkville
Victoria 3052
Australia
Tel: +613 9903 9067
Fax: +613 9903 9581
Email: arthur.christopoulos@med.monash.edu.au

Number of text pages: 41

Number of tables: 3

Number of figures: 8

Number of references: 40

Number of words in the Abstract: 248

Number of words in the Introduction: 733

Number of words in the Discussion: 1420

Abbreviations:

AC-42, 4-n-butyl-1-[4-(2-methylphenyl)-4-oxo-1-butyl] piperidine hydrogen chloride ; C_7/3-phth , heptane-1,7-bis-[dimethyl-3'-phthalimidopropyl]-ammonium bromide; 77-LH-28-1, 1-[3-(4-butyl-1-piperidinyl)propyl]-3,4-dihydro-2(1H)-quinolinone; McN-A-343, 4-*I*-[3-chlorophenyl]carbamoyloxy)-2-butynyltrimethylammnonium chloride; GPCR, G protein-coupled receptor; mAChR, muscarinic acetylcholine receptor; McN-A-343, 4-*I*-[3-chlorophenyl]carbamoyloxy)-2-butynyltrimethylammnonium chloride; [^{3}H]*N*-methylscopolamine, [^{3}H]NMS; pfu, plaque-forming units; [^{3}H]QNB, [^{3}H]quinuclidinyl benzilate; WT, wild type.

Molecular Pharmacology Fast Forward. Published on April 22, 2010 as DOI: 10.1124/mol.110.064345
This article has not been copyedited and formatted. The final version may differ from this version.

Abstract

Recent years have witnessed the discovery of novel selective agonists of the M_1 muscarinic acetylcholine (ACh) receptor (mAChR). One mechanism invoked to account for the selectivity of such agents is that they interact with allosteric sites. We investigated the molecular pharmacology of two such agonists, 1-[3-(4-butyl-1-piperidinyl)propyl]-3,4-dihydro-2(1H)-quinolinone (77-LH-28-1) and 4-n-butyl-1-[4-(2-methylphenyl)-4-oxo-1-butyl] piperidine hydrogen chloride (AC-42), at the wild type and three mutant M_1 mAChRs. Both agonists inhibited the binding of the orthosteric antagonist, [^{3}H]N-methylscopolamine ([^{3}H]NMS), in a manner consistent with orthosteric competition or high negative cooperativity. Functional interaction studies between 77-LH-28-1 and ACh also indicated a competitive mechanism. Dissociation kinetic assays revealed that the agonists could bind allosterically when the orthosteric site was pre-labeled with [^{3}H]NMS, and that 77-LH-28-1 competed with the prototypical allosteric modulator, heptane-1,7-bis-[dimethyl-3'-phthalimidopropyl]-ammonium bromide (C_7/3-phth) under these conditions. Mutation of the key orthosteric site residues, $Y^{381}A$ (transmembrane helix 6) and $W^{101}A$ (transmembrane helix 3), reduced the affinity of prototypical orthosteric agonists, but increased the affinity of the novel agonists. Divergent effects were also noted on agonist signaling efficacies at these mutants. We identified a novel mutation, $F^{77}I$ (transmembrane helix 2), which selectively reduced the efficacy of the novel agonists in mediating intracellular Ca^{++} elevation and phosphorylation of ERK1/2. Molecular modeling suggested a possible "bitopic" binding mode, whereby the agonists extend down into the orthosteric site as well as up towards extracellular receptor regions associated with an allosteric site. It is possible that this bitopic mode may explain the pharmacology of other selective mAChR agonists.

Molecular Pharmacology Fast Forward. Published on April 22, 2010 as DOI: 10.1124/mol.110.064345
This article has not been copyedited and formatted. The final version may differ from this version.

Introduction

The five mAChRs are prototypical Family A members of the G protein-coupled receptor (GPCR) superfamily and are widespread throughout the central nervous system and periphery (Christopoulos, 2007; Hulme et al., 1990; Wess et al., 2007). Based on anatomical, pharmacological, and preclinical animal model studies, the M_1 mAChR subtype has long been considered a potential therapeutic target for the treatment of cognitive deficits associated with disorders such as Alzheimer's disease and schizophrenia (Langmead et al., 2008b). Importantly, human clinical data derived from trials utilizing the M_1/M_4 mAChR-preferring mAChR agonist, xanomeline, have also provided evidence for cognitive improvement (Bodick et al., 1997; Shekhar et al., 2008). However, the development of truly subtype-selective mAChR agonists has been hampered by the very high degree of sequence homology within the orthosteric (acetylcholine-binding) site across all five mAChRs (Hulme et al., 1990).

It is now well established that mAChRs also possess topographically distinct allosteric binding sites that may offer a novel avenue towards attaining greater receptor subtype selectivity (Conn et al., 2009). Although early studies in this area focused on allosteric modulators, such as gallamine and C_7/3-phth, which regulated the actions of orthosteric ligands while lacking any appreciable intrinsic efficacy of their own (Gregory et al., 2007), recent progress has been made in identifying novel selective agonists that also display pharmacological characteristics suggestive of an allosteric mode of action. The best studied agonist in this regard is AC-42 (Fig. 1), which possesses significant functional selectivity for activating the M_1 mAChR relative to other subtypes (Spalding et al., 2002), interacts allosterically with the antagonists, [^{3}H]NMS and atropine (Langmead et al., 2006; Spalding et al., 2006), and is relatively insensitive to key mutations in the orthosteric binding pocket, such

Molecular Pharmacology Fast Forward. Published on April 22, 2010 as DOI: 10.1124/mol.110.064345
This article has not been copyedited and formatted. The final version may differ from this version.

as $Y^{106}A$, $Y^{381}A$ and $N^{382}A$ (residues 3.33, 6.51 and 6.52, respectively, using the Ballesteros and Weinstein, (1995) convention), which have profound inhibitory effects on the binding and/or function of the prototypical non-selective orthosteric agonist, carbachol (Spalding et al., 2006; Spalding et al., 2002). However, additional mutational analysis of key residues in transmembrane domain (TM) 3 of the rat M_1 mAChR identified $L^{102}A$ (3.29) as a mutation that inhibited the function of *both* carbachol *and* AC-42, and $W^{101}A$ (3.28) as a mutation that profoundly *increased* the function of AC-42, while *inhibiting* that of carbachol (Spalding et al., 2006). Thus, an interesting picture is emerging that suggests that novel agonists, such as AC-42, although clearly binding in a different mode to prototypical orthosteric agonists can still display sensitivity to some receptor epitopes commonly associated with the orthosteric binding pocket. One possible explanation for such findings may be that the novel agonists are "bitopic" ligands, being able to interact with regions in both orthosteric and allosteric sites, as has been demonstrated recently for the partial agonist, 4-*I*-[3-chlorophenyl]carbamoyloxy)-2-butynyltrimethylammnonium chloride (McN-A-343), at the M_2 mAChR (Valant et al., 2008).

More recently, we have described a new agonist, 77-LH-28-1 (Fig. 1), which is a structural analogue of AC-42 that also displays functional selectivity for the M_1 mAChR over other subtypes (Langmead et al., 2008a; May et al., 2007). 77-LH-28-1 is bioavailable, brain-penetrant and, importantly, displays higher efficacy than AC-42 when tested at native M_1 mAChRs (Langmead et al., 2008a). At the M_2 mAChR, 77-LH-28-1 can act as an allosteric modulator of [^{3}H]NMS dissociation kinetics (May et al., 2007), and a very recent study at the M_1 mAChR (Lebon et al., 2009) suggested a novel binding mode for both 77-LH-28-1 and AC-42 that may involve a conformational isomerization of the side-chain of W^{101} (3.28). Given the growing interest in such novel agonists of the M_1 mAChR, the current study aimed to investigate the pharmacological properties of 77-LH-28-1 at the M_1 mAChR in detail and

Molecular Pharmacology Fast Forward. Published on April 22, 2010 as DOI: 10.1124/mol.110.064345
This article has not been copyedited and formatted. The final version may differ from this version.

to compare them to AC-42, as well as the prototypic orthosteric agonists, ACh and pilocarpine. We also included a comparison of the effects on agonist affinity and efficacy of two key orthosteric site mutations, $W^{101}A$ (3.28) and $Y^{381}A$ (6.51), as well as a novel TM2 mutant, $F^{77}I$ (2.56), which had been suggested to affect the activity of AC-42 in preliminary studies (Jacobson et al., 2004). We reveal that 77-LH-28-1 can interact with part of the "common" allosteric binding site utilized by the prototypical modulator, C_7/3-phth, on a [^{3}H]NMS-occupied M_1 mAChR, and suggest a new role for F^{77} (2.56) at the top of TM2 of the M_1 mAChR in selectively controlling the efficacy of novel agonists such as 77-LH-28-1 and AC-42.

Molecular Pharmacology Fast Forward. Published on April 22, 2010 as DOI: 10.1124/mol.110.064345
This article has not been copyedited and formatted. The final version may differ from this version.

Materials and Methods

Materials

Chinese hamster ovary (CHO) Flp-In™ cells and Hygromycin B were purchased from Invitrogen (Carlsbad, USA). U2OS osteosarcoma cells were obtained from the ATCC (www.atcc.org). Dulbecco's Modified Eagle media (DMEM) and Fetal Bovine Serum (FBS) were from Gibco (Gaithersburg, USA) and JRH Biosciences (Lenexa, USA), respectively. The AlphaScreen™ SureFire™ phospho-ERK1/2 reagents were kindly donated by Dr. Michael Crouch (TGR Biosciences, South Australia), whilst the AlphaScreen streptavidin donor beads and anti-IgG (Protein A) acceptor beads used for pERK1/2 detection, [^{3}H]quinuclidinyl benzilate ([^{3}H]QNB) (specific activity 52 Ci/mmol) and [^{3}H]NMS (specific activity 72 Ci/mmol) were purchased from PerkinElmer (Massachusetts, USA). C_7/3-phth was synthesized in-house at Monash University by Dr. Celine Valant. AC-42 and 77-LH-28-1 were synthesized in-house at GlaxoSmithKline, Harlow, UK, as described previously (Langmead et al., 2008a; Acadia patent WO2003/057672). All other chemicals were from Sigma Chemical Company (St Louis, USA).

cDNA constructs and generation of stable cell lines

cDNA encoding the human M_1 mAChR was obtained from Missouri University of Science and Technology (www.cdna.org), and was used to generate CHO Flp-In cells stably expressing the receptor as described previously (Avlani et al., 2007; May et al., 2007). For experiments performed on U2OS cells, transient expression of wild-type and mutant M_1 mAChR constructs was achieved by infection with BacMam virus for 24 hr at varying transduction concentrations (plaque-forming units; pfu; Ames et al., 2007). To achieve this, the virus was mixed at the desired dilution (pfu/ml) with U2OS cell suspension immediately prior to plating/passaging of the cells. Modified baculovirus containing the mammalian

Molecular Pharmacology Fast Forward. Published on April 22, 2010 as DOI: 10.1124/mol.110.064345
This article has not been copyedited and formatted. The final version may differ from this version.

cytomegalovirus promoter was produced using the Bac-to-Bac Baculovirus expression system (Invitrogen, USA). Mutant receptor constructs were made using either the QuikChange site-directed mutagenesis kit (Stratagene, USA) or by the method of PCR gene splicing by overlap extension (Horton et al., 1990). The accuracy of all PCR-derived sequences was confirmed by dideoxy sequencing of the mutant plasmids.

Membrane preparation

CHO Flp-In M_1 cells were grown until approximately 90% confluent and harvested using 2 mM EDTA in phosphate buffered saline (PBS) (137 mM NaCl, 2.7 mM KCl, 4.3 mM Na_2HPO_4, 1.5 mM KH_2PO_4). Cells were pelleted by centrifugation for 10 min at 1,200 x g and the pellets were resuspended in 30 ml of buffer containing 20 mM HEPES and 10 mM EDTA at pH 7.4. All subsequent steps were performed at 4°C. The cell suspension was homogenized using a polytron PT 1200CL homogenizer, with 2 x 10 sec bursts separated by cooling on ice. The cell homogenate was centrifuged for 5 min at 1,700 x g and the supernatant was transferred to new tubes and further centrifuged (90 min, 38,000 x g) in a Sorval centrifuge. The pellet was resuspended in 10 ml buffer (20 mM HEPES, 0.1 mM EDTA, pH 7.4) and briefly homogenized to ensure uniform consistency. Membranes were aliquoted and stored at -80^{o}C. The protein concentration was determined by the method of Bradford using bovine serum albumin as a standard (Bradford, 1976).

Radioligand equilibrium binding assays

Saturation and competition binding assays were performed both in membranes derived from CHO FlpIn M_1 cells, as well as in intact U2OS cells transduced with either the M_1-WT, M_1-$Y^{381}A$, M_1-$W^{101}A$ or M_1-$F^{77}I$. For membrane-based saturation binding assays, 15 μg of CHO FlpIn M_1 membranes were incubated with the orthosteric antagonist, [^{3}H]NMS, in 1 ml

Molecular Pharmacology Fast Forward. Published on April 22, 2010 as DOI: 10.1124/mol.110.064345
This article has not been copyedited and formatted. The final version may differ from this version.

HEPES buffer (20 mM HEPES, 100 mM NaCl, 10 mM $MgCl_2$, pH 7.4) at 37°C for 1 hr prior to termination of the assay by rapid filtration onto GF/B grade filter paper using a Brandel harvester, followed by 3 x 2 ml washes with ice-cold NaCl (0.9%). Nonspecific binding was defined in the presence of 10 μM atropine and radioactivity was determined by liquid scintillation counting. For inhibition binding assays, membranes were incubated in HEPES buffer containing increasing concentrations of the allosteric modulator, C_7/3-phth, or either of the novel agonists, 77-LH-28-1 or AC-42, for 1 hr at 37°C in the presence of a [^{3}H]NMS concentration approx. equal to its equilibrium dissociation constant, unless specified otherwise in the Results. Non-specific binding, reaction termination and radioactivity determination were as described above.

For binding assays performed on intact U2OS cells, cells were first transduced with various amounts of plaque forming units (0.5 or 1.25 pfu/ml as indicated in Tables 1-3) and, 24 hr later, were harvested by trypsinization and resuspended in Ca^{++} assay buffer (150 mM NaCl, 2.6 mM KCl, 1.18 mM $MgCl_2$, 10 mM D-Glucose 10 mM HEPES, 2.2 mM $CaCl_2$, 0.5% BSA & 2.5 mM probenecid). For saturation binding experiments, the U2OS cells were incubated in 1 ml total volume of Ca^{++} buffer containing 100,000 cells/ml and concentrations of [^{3}H]QNB ranging from 0.002 nM to 0.5 nM for 60 min at 37°C. For competition binding experiments, the cells were incubated in 1 ml total volume of Ca^{++} buffer containing 0.1nM [^{3}H]QNB and a range of concentrations of the ACh, pilocarpine, AC-42 or 77-LH-28-1, for 30 min at 37°C. Non-specific binding was defined using 10 μM atropine. Incubation was terminated by rapid filtration through Whatman GF/C filters using Brandel cell harvester (Gaithersburg, MD). All other details were as described above.

Molecular Pharmacology Fast Forward. Published on April 22, 2010 as DOI: 10.1124/mol.110.064345
This article has not been copyedited and formatted. The final version may differ from this version.

[^{3}H]NMS dissociation kinetic assays

CHO-FlpIn cell membranes (15 μg) were equilibrated with [^{3}H]NMS (0.5 nM) in a 1 ml total volume of HEPES buffer (also containing 100 μM Gpp(NH)p) for 60 min at 37°C. Atropine (10 μM) alone or in the presence of test ligand was then added at various time points to prevent the re-association of [^{3}H]NMS with the receptor. In subsequent experiments designed to investigate the effect of a range of modulator concentrations on [^{3}H]NMS dissociation rate, a "two-point kinetic" experimental paradigm was used, where the effect of increasing concentrations of allosteric modulator on [^{3}H]NMS dissociation was determined at 0 and 10 min. This approach is valid to determine [^{3}H]NMS dissociation rate constants if the full time course of radioligand dissociation is monophasic both in the absence and presence of modulator (Kostenis and Mohr, 1996; Lazareno and Birdsall, 1995); this was the case in our current study. Termination of the reaction and determination of radioactivity were performed as described above.

U2OS cell intracellular calcium elevation assays

U2OS cells were transduced as described above and plated at a density of 50,000 cells/well in 96-well clear flat bottom plate. After 22 hr at 37°C, 5% CO_2, the cells were washed twice with Ca^{++} assay buffer and loaded with Ca^{++} assay buffer containing 10 μM Fluo-4 and incubated in dark. The cells were then washed twice with Ca^{++} buffer to remove excess Fluo-4. The calcium elevation in response to addition increasing concentrations of ligand was measured for 3 min at 1.5 sec intervals using a Flexstation (Molecular Devices). For functional interaction studies, cells were incubated at 37°C with varying concentrations of ACh in the absence and presence of different concentrations of a second compound (see Results), which was added 60 sec prior to the addition of ACh for a further 120 sec. Calcium elevation was measured using Flexstation at an interval of 1.5 sec for a total of 195 sec.

Molecular Pharmacology Fast Forward. Published on April 22, 2010 as DOI: 10.1124/mol.110.064345
This article has not been copyedited and formatted. The final version may differ from this version.

U2OS cell extracellular signal regulated kinase 1/2 phosphorylation (pERK1/2) assays

Initial ERK1/2 phosphorylation time-course experiments were performed to determine the time at which ERK1/2 phosphorylation was maximal following stimulation by each agonist. Cells were seeded into transparent 96-well plates at 40,000 cells per well and grown overnight or until confluent. Cells were then washed twice with PBS and incubated in serum-free DMEM at 37^{o}C for at least 4 hr to allow FBS-stimulated phosphorylated ERK1/2 (pERK1/2) levels to subside. Cells were stimulated with agonist using a staggered addition approach. For subsequent agonist-stimulated concentration-response experiments, cells were incubated at 37°C with each agonist for the 8 min required to achieve peak response. For all experiments, 10% FBS was used as a positive control, whilst vehicle controls were also performed. The reaction was terminated by removal of drugs and lysis of cells with 100 µl SureFire™ lysis buffer (as provided by the manufacturer). The lysates were agitated for 1-2 min and were diluted at a ratio of 4:1 v/v lysate:Surefire™ activation buffer in a total volume of 50 µl. Under low light conditions a 1:240 v/v dilution of AlphaScreen™ beads: Surefire™ reaction buffer was prepared and this was mixed with the activated lysate mixture in a ratio of 6:5 v/v, respectively, in a 384-well opaque Optiplate™. Plates were incubated in the dark at 37°C for 1.5 hr before the fluorescence signal was measured using a Fusion-α™ plate reader (PerkinElmer) using standard AlphaScreen™ settings.

Construction of an M_1 mAChR model

The initial model of the TM domain of the human M_1 mAChR was constructed by homology with the published X-ray crystal structure of β_2 adrenergic receptor 2RH1 (Cherezov et al., 2007). Alignment between the M_1 mAChR sequence and β_2 receptor was based on the "classical" motifs found in each TM region, such as the asparagine in TM1, the aspartate in

Molecular Pharmacology Fast Forward. Published on April 22, 2010 as DOI: 10.1124/mol.110.064345
This article has not been copyedited and formatted. The final version may differ from this version.

TM2, the "DRY" motif of TM3, the tryptophan in TM4, and the conserved prolines in TM5, TM6 and TM7. This alignment was used, with the standard homology modeling tools in the Quanta program (Accelerys Software, San Diego) to construct the seven helical bundle domain of the M_1 mAChR. The extracellular loop regions were subsequently added using a procedure developed in-house at GlaxoSmithKline, which makes use of a combined distance geometry sampling and molecular dynamics simulation (Blaney et al., 2001). The sidechains of this model were then refined using the Karplus standard rotamer library (Dunbrack and Karplus, 1993). The final model was optimized fully (500 steps of Steepest Descent (SD) followed by 5000 steps of Adopted Basis Newton Raphson (ABNR)) using the CHARMm force field. Helical distance constraints between the i^{th} and $i+4^{th}$ residues (except proline) within a range of 1.8Å-2.5Å, were used to maintain the backbone hydrogen bonds of the helix bundles.

Ligand docking studies

AC-42 and 77-LH-28-1 were docked into the receptor model manually using a variety of low energy starting conformations. Adjustments of the receptor protein sidechains were made where necessary, always ensuring that these sidechains were only in allowed rotameric states (Dunbrack and Karplus, 1993). Once again, full optimization of the receptor-ligand complexes was performed using CHARMm, the only constraints used being those that maintained the hydrogen bonding pattern of the helical bundle. This procedure allows full relaxation of both the ligand and the whole protein, something that is not possible with automated docking procedures. Although numerous binding orientations were found to be possible, one docked binding mode that accommodated both novel agonists satisfied much of the site-directed mutagenesis data generated.

Molecular Pharmacology Fast Forward. Published on April 22, 2010 as DOI: 10.1124/mol.110.064345
This article has not been copyedited and formatted. The final version may differ from this version.

Data analysis

All data were analyzed using Prism 5.01 (GraphPad Software, San Diego, USA). For radioligand saturation binding data, the following equation was globally fitted to non-specific and total binding data:

$$Y = \frac{B_{max} \cdot [A]}{[A] + K_A} + NS \cdot [A] \qquad (1)$$

where Y is radioligand binding, B_{max} is the total receptor density, [A] is the radioligand concentration, K_A is the equilibrium dissociation constant of the radioligand and NS is the fraction of nonspecific radioligand binding.

For radioligand inhibition binding experiments a one-site binding equation (2) was fitted to the specific binding of each orthosteric ligand:

$$Y = \frac{(\text{Top-Bottom})}{1 + 10^{(\log[B] - \log IC_{50})}} + \text{Bottom} \qquad (2)$$

where Top and Bottom are the maximal and minimal asymptotes of the curve, respectively, log[B] is the concentration of inhibitor and $\log IC_{50}$ is the logarithm of the concentration of inhibitor that reduces half the maximal radioligand binding for each binding site. IC_{50} values were converted to K_A values (inhibitor equilibrium dissociation constant) using the Cheng and Prusoff (1973) equation.

For some experiments, as indicated in the Results, the following version of a simple allosteric ternary complex model (Lazareno and Birdsall, 1995) was also fitted to inhibition binding data:

Molecular Pharmacology Fast Forward. Published on April 22, 2010 as DOI: 10.1124/mol.110.064345
This article has not been copyedited and formatted. The final version may differ from this version.

$$\frac{Y}{Y_{max}} = \frac{[A]}{[A] + \frac{K_A\left(1 + [B]/K_B\right)}{\left(1 + \alpha[B]/K_B\right)}} \qquad (3)$$

where Y/Y_{max} denotes fractional specific binding, [A] and K_A are as defined above for equation (1), K_B denotes the allosteric modulator dissociation constant and α denotes the cooperativity factor. Values of $\alpha > 1$ denote positive cooperativity, values < 1 (but greater than 0) denote negative cooperativity, values = 1 denote neutral cooperativity and values approaching zero denote inhibition that is indistinguishable from competitive (orthosteric) antagonism.

Dissociation kinetic data all followed a monoexponential decay. Thus, the following equation was fitted to these data:

$$B_t = B_0 \cdot e^{-k_{off} \times t} \qquad (4)$$

where t denotes incubation time, B_t denotes specific radioligand binding at time t, B_0 denotes the specific radioligand binding at time at equilibrium (time = 0) and k_{off} represents the observed radioligand dissociation rate constant. For the two-point dissociation experiments, where the effects of a range of concentrations of allosteric modulators were investigated, individual k_{off} values determined in the presence of modulator were normalized to the control k_{off} value (absence of modulator) and then plotted as a function of modulator concentration.

The following three-parameter logistic equation was fitted to concentration-response data generated from the functional U2OS cell-based assays:

Molecular Pharmacology Fast Forward. Published on April 22, 2010 as DOI: 10.1124/mol.110.064345
This article has not been copyedited and formatted. The final version may differ from this version.

$$E=Bottom+\frac{E_{max}\text{-}Bottom}{1+10^{(-pEC_{50}-[A])}} \qquad (5)$$

where E is response, E_{max} and Bottom are the top and bottom asymptotes of the curve, respectively, [A] is the agonist concentration and pEC_{50} is the negative logarithm of the agonist concentration that gives a response halfway between E_{max} and Bottom. Where appropriate, the following form of an operational model of agonism (Black and Leff, 1983) was also fitted to agonist data:

$$Y=Basal+\frac{E_m\text{-}Basal}{1+\left[\frac{10^{\log K_A}+10^{\log[A]}}{10^{\log\tau}\times 10^{\log[A]}}\right]} \qquad (6)$$

where E_m is the maximal possible response of the system (not the agonist), Basal is the basal level of response in the absence of agonist, K_A denotes the functional equilibrium dissociation constant of the agonist (A), τ is an index of the coupling efficiency (efficacy) of the agonist and is defined as R_T/K_E where R_T is the total concentration (B_{max}) of receptors and K_E is the concentration of agonist-receptor complex that yields half the maximum system response (E_m). Throughout this study, all references to the term "efficacy" specifically relate to the property quantified by τ. To define the E_m and τ for each mutant and assay, the K_A for each agonist was constrained to equal the K_A value derived from radioligand binding assays (see *Results*) in the nonlinear regression procedure. In addition, because the τ parameter can be influenced by variations in the expression level of various receptor constructs, the values reported in this study have been normalized according to the following ratio: $\tau_{corrected}$ (τ_C) = $\tau_{estimated} \times (B_{max\text{-}mutant}/B_{max\text{-}wildtype})$ (see Gregory et al., 2010).

Molecular Pharmacology Fast Forward. Published on April 22, 2010 as DOI: 10.1124/mol.110.064345
This article has not been copyedited and formatted. The final version may differ from this version.

A logistic equation of competitive agonist-antagonist interaction (Motulsky and Christopoulos, 2004) was globally fitted to data from functional experiments measuring the interaction between ACh and atropine:

$$\text{Response}=\text{Bottom}+\frac{(E_{max}\text{-Bottom})}{1+\left(\frac{10^{-pEC_{50}}\left[1+\left(\frac{[B]}{10^{-pA_2}}\right)^{s}\right]}{[A]}\right)} \quad (7)$$

where s represents the Schild slope for the antagonist, and pA_2 represents the negative logarithm of the molar concentration of antagonist that makes it necessary to double the concentration of agonist needed to elicit the original submaximal response obtained in the absence of antagonist; all other parameters are as defined above in equation 5. The following operational model for the competitive interaction between an orthosteric full and partial agonist, as derived previously by (Leff et al., 1993), was also fitted to the interaction data between ACh and 77-LH-28-1:

$$E=\frac{E_m\left([A]K_B+\tau[B][EC_{50}]\right)^n}{[EC_{50}]^n\left(K_B+[B]\right)^n+\left([A]K_B+\tau[B][EC_{50}]\right)^n} \quad (8)$$

where the parameters are as described above for equations 6 and 7.

All parametric measures of potency, affinity, operational efficacy and cooperativity were estimated as logarithms (Christopoulos, 1998). In all instances, models were fitted to pooled datasets. Statistical comparisons between parameters were performed using Student t-test or F-test, where appropriate, with $p < 0.05$ taken as indicating significance.

Molecular Pharmacology Fast Forward. Published on April 22, 2010 as DOI: 10.1124/mol.110.064345
This article has not been copyedited and formatted. The final version may differ from this version.

Results

77-LH-28-1 and AC-42, inhibit the binding of the orthosteric antagonist, [^{3}H]NMS at the M_1 mAChR

AC-42 and 77-LH-28-1 were initially studied using an equilibrium binding assay to examine their interaction with the radioligand, [^{3}H]NMS (pK_A = 9.7 ± 0.3; B_{max} = 4.5 ± 1.3 pmol/mg; n = 3). Both compounds inhibited binding in a monophasic manner almost down to non-specific levels at [^{3}H]NMS concentrations of 0.2 nM (data for 77-LH-28-1 shown in Figure 2A). In order to reveal any potential allosteric mechanism of action, the same experiment was performed using 2 nM [^{3}H]NMS (equivalent to approximately 10 x K_A). Global analysis of both datasets according to Equation 3 (Materials & Methods) indicated that the compounds possessed micromolar affinity for the M_1 mAChR with high degrees of negative cooperativity with respect to [^{3}H]NMS (77-LH-28-1: pK_B = 6.34 ± 0.14; Log α = -1.78 ± 0.17 (α = 0.017; n = 3); AC-42: pK_B = 5.87 ± 0.06; Log α = -2.03 ± 0.06 (α = 0.009; n = 3). In contrast, the prototypical mAChR allosteric modulator, C_7/3-phth, displayed much weaker negative cooperativity, as evidenced by its inability to fully inhibit specific radioligand binding at even 0.2 nM (Figure 2B; C_7/3-phth: pK_B = 5.53 ± 0.04 ; Logα = -0.81 ± 0.02 (α = 0.15; n = 3)).

77-LH-28-1 recognizes part of the "common" allosteric site on the [^{3}H]NMS-occupied M_1 mAChR

Due to the high degree of negative cooperativity observed between [^{3}H]NMS and AC-42 or 77-LH-28-1, the conclusion that these agonists interact allosterically with respect to NMS at the M_1 mAChR was equivocal. In order to validate their mechanism of action further, their effects on the dissociation of a pre-formed complex of M_1 mAChR and [^{3}H]NMS was examined. In the absence of allosteric modulator, [^{3}H]NMS dissociation was rapid and

Molecular Pharmacology Fast Forward. Published on April 22, 2010 as DOI: 10.1124/mol.110.064345
This article has not been copyedited and formatted. The final version may differ from this version.

monophasic, with a k_{off} value of 0.35 ± 0.01 min^{-1} (n=3). The presence of C_7/3-phth (100 μM) significantly slowed the [^{3}H]NMS dissociation rate (Figure 3A; k_{off} = 0.04 ± 0.01 min^{-1}), consistent with previous observations of its allosteric mechanism of action. Similarly, 100 μM of either AC-42 (k_{off} = 0.28 ± 0.01 min^{-1}) or 77-LH-28-1 (k_{off} = 0.22 ± 0.01 min^{-1}) significantly retarded the rate of [^{3}H]NMS dissociation from the M_1 mAChR compared to control, although not to the same extent as observed with C_7/3-phth ($P < 0.05$; one-way ANOVA followed by Dunnett's post test; Figure 3A). These effects clearly show that both AC-42 and 77-LH-28-1 are able to interact allosterically with the [^{3}H]NMS-occupied receptor.

We then used a "two-point kinetic" experimental paradigm (Kostenis and Mohr, 1996), to determine the concentration-dependence of the effect of C_7/3-phth on [^{3}H]NMS dissociation rate, which allowed for an estimate of its potency at the [^{3}H]NMS-occupied receptor, pIC_{50} = 4.77 ± 0.06 (n = 3; Figure 3B). Unfortunately, it was not possible to establish a similar concentration-response profile for either AC-42 or 77-LH-28-1 due to a combination of their low solubility and the relatively modest effect they have on [^{3}H]NMS dissociation rate. However, it was possible to probe the interaction between C_7/3-phth and 77-LH-28-1 using this experimental design. As shown in Figure 3B, 77-LH-28-1 (300 μM) produced a significant 6-fold rightward shift in the concentration-response curve of C_7/3-phth to inhibit the rate of [^{3}H]NMS dissociation (pIC_{50} in the presence of 77-LH-28-1 = 3.99 ± 0.14; n = 3) as well as exerting an effect to slow [^{3}H]NMS dissociation in its own right. Assuming a competitive interaction, this corresponds to a pA_2 value of 4.3 for 77-LH-28-1. According to the allosteric ternary complex model, this pA_2 value corresponds to the negative log of the dissociation constant of 77-LH-28-1 for the [^{3}H]NMS-occupied receptor, which we can also calculate separately from the K_B and α values derived from Equation 4 above (yielding a predicted pA_2 value of 4.6). These data indicate, for the first time, that 77-LH-28-1 likely

Molecular Pharmacology Fast Forward. Published on April 22, 2010 as DOI: 10.1124/mol.110.064345
This article has not been copyedited and formatted. The final version may differ from this version.

shares some of its binding site with that of the prototypical mAChR allosteric modulator, C_7/3-phth (at the [^{3}H]NMS-occupied receptor).

Determination of functional efficacies and interactive properties of novel agonists at the M_1 mAChR

To evaluate the functional pharmacology of AC-42 and 77-LH-28-1 in comparison with prototypical orthosteric agonists, intracellular calcium elevation studies were performed in U2OS cells transiently transduced with the M_1 mAChR using BacMam (modified baculovirus) technology. One advantage of BacMam transductions is that transient receptor expression level can be controlled by varying the multiplicity of infection during the transduction. Figure 4A shows the effect of varying transduction concentrations (0.5, 2 and 8 pfu per cell) on the concentration–response curve to ACh, indicating that different receptor expression levels allow for clear separation of agonist efficacies. 2 pfu / cell was chosen as an optimal multiplicity of infection for allowing ACh to elicit a close to system-maximal Ca^{++} response. These conditions clearly revealed that 77-LH-28-1 and AC-42 were lower efficacy agonists than ACh; pilocarpine was included as a prototypical orthosteric partial agonist comparator (Figure 4B).

Subsequently, we transduced U2OS cells with 0.5 pfu / cell to reduce receptor expression, and hence agonist efficacy, to study the functional interaction between 77-LH-28-1 and ACh; the prototypical orthosteric antagonist, atropine, was included as a comparator. The effects of atropine and 77-LH-28-1 on the ACh concentration-response curve are shown in Figure 5. Increasing concentrations of both atropine and 77-LH-28-1 produced concentration-dependent, parallel, rightward shifts in the ACh concentration-response curve. In addition, a slightly elevated basal response was observed in the presence of 77-LH-28-1, indicative of the residual partial agonist activity of this compound. Analysis of the ACh/atropine data

Molecular Pharmacology Fast Forward. Published on April 22, 2010 as DOI: 10.1124/mol.110.064345
This article has not been copyedited and formatted. The final version may differ from this version.

according to equation 7 (Materials & Methods), and the ACh/77-LH-28-1 data according to equation 8, yielded Schild slopes not significantly different from unity (0.97 ± 0.05 for atropine and 0.85 ± 0.11 for 77-LH-28-1); constraining them as such yielded the following pA_2 values of 9.30 ± 0.08 (n = 5) for atropine and 6.21 ± 0.12 (n = 4) for 77-LH-28-1, respectively. Therefore, the interaction between 77-LH-28-1 and ACh, at least under the conditions tested, appears indistinguishable from simple competition, suggesting that the binding of 77-LH-28-1 must either overlap with that of the orthosteric site or be linked to the binding of ACh with a very high degree of negative cooperativity that could not be differentiated from orthosteric competition over the concentration range tested in the calcium assay.

Effects of key M_1 mAChR mutations on agonist pharmacology

The preceding studies indicated that the novel agonists display pharmacology that is consistent with both orthosteric and allosteric modes of action, depending on the experimental design. It is possible that such compounds recognize epitopes in both these regions of the receptor, and adopt more than one binding pose depending on whether the orthosteric site is occupied by another ligand or not. To further probe these interactions at the molecular level, we examined the pharmacology of the novel agonists at M_1 mAChRs containing key point mutations. Specifically, we determined the affinity and efficacy of AC-42 and 77-LH-28-1 at $Y^{381}A$, $W^{101}A$ and $F^{77}I$ mutant M_1 mAChRs. Y^{381} in TM6 is a known key component of the ACh orthosteric binding site that, when mutated to alanine, reduces the potency of prototypical orthosteric agonists such as ACh and carbachol while having relatively little effect on the response to novel agonists such as AC-42 and N-desmethylclozapine (Spalding et al., 2002; Sur et al., 2003; Ward et al., 1999). W^{101} in TM3 of the M_1 mAChR has previously been shown to be part of a 'second-shell' of residues that surround the orthosteric binding site (Hulme et al., 2003), and $W^{101}A$ mutation markedly increases the potency of

Molecular Pharmacology Fast Forward. Published on April 22, 2010 as DOI: 10.1124/mol.110.064345
This article has not been copyedited and formatted. The final version may differ from this version.

structurally-related, selective agonists such as AC-260584 (Spalding et al., 2006) and 77-LH-28-1 (Lebon et al., 2009) at the receptor. Finally, F^{77} was identified in preliminary work as a residue which, when mutated to isoleucine, caused a reduction in the potency of AC-42 (Jacobson et al., 2004).

U2OS cells were transduced with different pfu/cell in order to attain roughly similar levels of receptor expression for mutant versus wild type receptors, as determined by whole cell [^{3}H]QNB binding (Table 1); we used this radioligand because its affinity is substantially less affected by mutation of key residues, such as $W^{101}A$ and $Y^{381}A$, compared to the binding of [^{3}H]NMS (Ward et al., 1999; Lebon et al. 2009). Although there were still variations in expression noted between mutants, the estimated B_{max} values were used to correct for these variations after application of an operational model of agonism (equation 6) to obtain agonist efficacy estimates ($Log\tau_c$ values, Table 2) for Ca^{++} elevation. [^{3}H]QNB and the agonists tested each displayed affinities at the wild-type M_1 mAChR consistent with their previously described pharmacology at this receptor subtype. The $W^{101}A$ mutation resulted in a small, but significant, reduction in affinity of ACh, pilocarpine and [^{3}H]QNB (Table 1), consistent with a role for W^{101} as part of the 'second-shell' of residues forming the orthosteric binding site. Conversely, this mutation resulted in significant increases in the affinity of AC-42 and 77-LH-28-1 (Table 1), in agreement with previous binding studies (Lebon et al., 2009). Interestingly, this mutation did not alter the efficacies of ACh and pilocarpine (Table 2; Fig. 6), but enhanced the efficacy of AC-42 (though not 77-LH-28-1).

Mutation of $Y^{381}A$ in TM6 did not result in a change of [^{3}H]QNB affinity (Table 1), consistent with previous observations that this residue is able to discriminate between the binding of [^{3}H]QNB and [^{3}H]NMS (Ward et al., 1999). However, mutation of $Y^{381}A$ markedly reduced the affinity of orthosteric agonists ACh and pilocarpine, consistent with its

Molecular Pharmacology Fast Forward. Published on April 22, 2010 as DOI: 10.1124/mol.110.064345
This article has not been copyedited and formatted. The final version may differ from this version.

role as a key binding partner in the orthosteric agonist binding site. This mutation also reduced ACh and pilocarpine efficacy, suggesting that Y^{381} is also involved in receptor activation by orthosteric agonists (Table 2; Fig. 6). Similarly, Y^{381}A reduced the efficacies of AC-42 and 77-LH-28-1, but moderately increased their affinity compared to the wild-type receptor, suggesting that whilst the role of Y^{381} in receptor activation may be common to all the agonists tested, only orthosteric agonists rely on this residue for binding to the receptor.

F^{77} is located in TM2, and had been reported in a preliminary study to selectively diminish the potency of AC-42 when mutated to isoleucine (Jacobson et al., 2004). We have now found that this mutation did not alter the affinity of any of the ligands tested (with the exception of a small reduction in 77-LH-28-1 affinity; Table 1). However, the efficacies (Log τ_c values) of both AC-42 and 77-LH-28-1 were substantially reduced by F^{77}I, whereas those of ACh and pilocarpine were unaltered (Table 2; Fig. 6). This indicates that mutation of F^{77}I selectively affects the ability of AC-42 and 77-LH-28-1 to signal, unlike the Y^{381}A mutation, which reduced the efficacy of all the agonists tested.

To further verify this novel observation, the activity of all four agonists was examined at both the wild-type and F^{77}I constructs in a second signaling assay, that of ERK1/2 phosphorylation. All agonists displayed Logτ_c values somewhat lower than those observed in the Ca^{++} assay (Table 3; Fig. 7), suggesting that the receptor coupling efficiency in the pERK1/2 assay is lower. In agreement with the previous dataset, mutation of F^{77} did not alter the efficacy of ACh or pilocarpine, but reduced the efficacy of 77-LH-28-1 and abolished the agonist activity of AC-42 (Table 3; Fig. 7). Thus the selective modulation of the efficacy of the novel agonists by F^{77}I was not restricted to a single pathway but observed for both Ca^{++} elevation and ERK1/2 phosphorylation.

Molecular Pharmacology Fast Forward. Published on April 22, 2010 as DOI: 10.1124/mol.110.064345
This article has not been copyedited and formatted. The final version may differ from this version.

Modeling and Ligand Docking

In addition to the radioligand binding and functional studies, molecular modeling and ligand docking were performed to rationalize the results seen with AC-42 and 77-LH-28-1. All reasonable docking solutions suggested that the aspartate residue (D^{105}) in TM3 was forming a charge-charge interaction with the protonated nitrogen of 77-LH-28-1. This placed the aromatic benzoyl portion of 77-LH-28-1 between helices 2, 3 and 7, with the phenyl ring adjacent to the flipped-out tryptophan (W^{101}) and encircled by a number of other aliphatic and aromatic residues: W^{91}, L^{102}, Y^{82} and Y^{85}. The butyl linker between the aromatic ring and the piperidine ring transverses a hydrophobic region defined by Y^{82}, L^{83}, L^{102} and I^{180} and the piperidine ring is interacting with S^{78} and Y^{404}. The aliphatic butyl tail of AC-42 is located deep within the receptor and is forming hydrophobic interactions with I^{74}, W^{378} and C^{407}. Interestingly, the phenylalanine residue F^{77}, located on the external side of TM2, does not appear to be interacting with the ligand; it does however appear to be playing a role in the stabilisation of the flipping of W^{101} by forming a π-π stacking interaction when W^{101} is in its flipped out gauche negative state. 77-LH-28-1 sits some distance from Y^{381} in TM6, consistent with previous reports of a lack of effect of mutation of this residue on AC-42 function (Spalding et al., 2002). The tyrosine residue Y^{381} is behind the Y^{404} residue on TM7 that is only partly in contact with the piperidine portion of 77-LH-28-1.

Molecular Pharmacology Fast Forward. Published on April 22, 2010 as DOI: 10.1124/mol.110.064345
This article has not been copyedited and formatted. The final version may differ from this version.

Discussion

The past decade has witnessed a virtual renaissance in the pharmacology of mAChR agonists, spearheaded by the discovery of compounds such as AC-42, which preferentially activate the muscarinic M_1 mAChR subtype (Langmead et al., 2006; Spalding et al., 2002). Importantly, a common mechanism invoked to explain the functional selectivity of these agonists has been one involving the possibility that they are allosteric (Jones et al., 2008; Langmead et al., 2006; Spalding et al., 2006; Sur et al., 2003). Our current findings suggest that these novel agonists indeed adopt different poses within the M_1 mAChR relative to prototypical orthosteric agonists such as ACh, but that they are unlikely to result in a purely allosteric mode of action.

It is of note that in previous studies (Langmead et al., 2006; Lebon et al., 2009), and in our current study, the interactions between 77-LH-28-1 or AC-42 with orthosteric antagonists were consistently characterized by very high degrees of negative cooperativity (Log α values $\geq$ -2), as determined by application of an allosteric ternary complex model to the data. Such highly negative allosteric interactions are virtually indistinguishable from a competitive interaction at equilibrium. This is in contrast to prototypical allosteric modulators, such as C_7/3-phth, which can be shown to interact via a purely allosteric mode in both equilibrium (Figure 2B) and kinetic (Figure 3) studies. The ability of ligands such as C_7/3-phth and 77-LH-28-1 to alter the dissociation rate of an orthosteric ligand is a key indicator of an allosteric interaction, but it should be noted that this type of assay monitors interactions on a receptor that has been pre-labeled with an orthosteric radioligand; dissociation kinetic experiments can reveal whether a ligand is able to adopt an allosteric binding pose, but cannot be used to conclude that this pose is relevant to a receptor that does not have an orthosteric ligand present. Indeed, functional interaction studies utilizing 77-LH-28-1 were in agreement with the equilibrium binding studies in that the interaction between this agent and the orthosteric agonist, ACh, were consistent with a simple competitive mechanism (Figure 5), or very high

Molecular Pharmacology Fast Forward. Published on April 22, 2010 as DOI: 10.1124/mol.110.064345
This article has not been copyedited and formatted. The final version may differ from this version.

negative cooperativity. This finding also complements previous data that showed the functional interaction between 77-LH-28-1 and scopolamine or pirenzepine were indistinguishable from simple competition (Langmead et al., 2008a). Although our finding of apparent competition between 77-LH-28-1 and C_7/3-phth on the [^{3}H]NMS-occupied receptor indicates that the novel agonist has the capacity to recognize epitopes that constitute the prototypical allosteric binding site on the M_1 mAChR, the log. affinity of the agonist for the occupied receptor (approx. 4.3) is markedly lower than its log. affinity for the free receptor (approx. 6.3). Given that the novel agonists have a much lower affinity for the allosteric site on the M_1 mAChR when the receptor is occupied by orthosteric ligand, it is unlikely that their purely allosteric properties will play a prominent role in their pharmacological effects at concentrations that are physiologically relevant.

Overall, the profile of behaviors exhibited by the novel agonists are qualitatively and quantitatively similar to that displayed by the mAChR partial agonist, McN-A-343, whose mechanism of action was the subject of debate in the literature (Birdsall et al., 1983; Christopoulos and Mitchelson, 1997; May et al., 2007). More recently, radioligand binding, functional and mutagenesis studies utilizing fragments of McN-A-343 revealed it to be a 'bitopic' ligand, namely, a hybrid molecule capable of interacting concomitantly with the receptor via both orthosteric and allosteric sites (Valant et al., 2008). This is a mode of interaction that is distinct from a 'pure' allosteric mode. Due to its recognition of epitopes within the orthosteric pocket, McN-A-343 appears competitive in equilibrium binding or functional assays, but utilizes regions of the allosteric site to derive functional selectivity; when the orthosteric site is pre-bound with radioligand, it adopts a second, purely allosteric binding mode, with much lower affinity. Given the parallels in the pharmacology, this may be a likely mechanism by which 77-LH-28-1 interacts with the unoccupied muscarinic M_1 mAChR, and one we have proposed for this agonist at the M_2 mAChR (Gregory et al., 2010).

Molecular Pharmacology Fast Forward. Published on April 22, 2010 as DOI: 10.1124/mol.110.064345
This article has not been copyedited and formatted. The final version may differ from this version.

Our modeling and ligand docking also support the notion that 77-LH-28-1 and AC-42 are bitopic ligands (Valant et al., 2008; Valant et al., 2009). Both agonists have basic centres that are likely to interact with D^{105} in the orthosteric binding site; previous mutational data support the requirement of this residue for receptor activation by these agonists (Lebon et al., 2009). However, the benzoyl aromatic group of 77-LH-28-1 is predicted to occupy space between TM domains 2, 3 and 7, close to the extracellular loops. Interestingly, W^{101} is thought to form the base of the binding site for the prototypical allosteric modulators such as C_7/3-phth (Matsui et al., 1995). This binding mode would explain the observation that 77-LH-28-1 appears to compete (at least in part) for the same binding site as C_7/3-phth (Figure 3B). It is likely that interactions in this region are responsible for the observed allosteric effects of 77-LH-28-1 when the receptor is pre-bound with [^{3}H]NMS. When the receptor is simultaneously exposed to 77-LH-28-1 and either [^{3}H]NMS (equilibrium binding) or ACh (functional Ca^{++} studies), the interaction of 77-LH-28-1 appears competitive, primarily due to the interaction with D^{105}.

The residues chosen for mutagenesis, W^{101}, Y^{381} and F^{77}, also proved useful in identifying patterns of behavior that can be used to differentiate prototypical orthosteric agonists from novel selective agonists (including putative bitopic agonists). The first two residues were selected as their mutation has been shown to have divergent effects on orthosteric and putatively allosteric agonists (Lebon et al., 2009; Spalding et al., 2006; Spalding et al., 2002), although their precise in role in ligand binding and receptor activation have not been fully established. F^{77} was highlighted as a residue which, when mutated to isoleucine, caused a reduction in the potency of AC-42 to activate the muscarinic M_1 mAChR (Jacobson et al., 2004). W^{101}, when in the gauche negative state, is predicted to be adjacent to the phenyl ring of 77-LH-28-1. Mutation of this residue to alanine has been shown to increase the potency of

Molecular Pharmacology Fast Forward. Published on April 22, 2010 as DOI: 10.1124/mol.110.064345
This article has not been copyedited and formatted. The final version may differ from this version.

AC-42 and related compounds (Spalding et al., 2006). The same mutation significantly reduced ACh and pilocarpine affinity but significantly *enhanced* AC-42 and 77-LH-28-1 affinity (Table 1); there was no change in agonist efficacy with the exception of a reduction in the Logτ_c value for AC-42 (Table 2). These data suggest that W^{101} primarily plays a role in the binding of 77-LH-28-1, probably by 'flipping out' to accommodate the ligand; therefore the absence of the side chain reduces the free energy required for ligand binding.

Mutation of $Y^{381}A$ significantly reduced the affinity of pilocarpine and ACh for the M_1 receptor (Table 1), consistent with a role in the orthosteric binding site (Ward et al., 1999). Interestingly, this mutation moderately increased the affinity of AC-42 and 77-LH-28-1 (Table 1) but significantly reduced the efficacy of all agonists tested (Table 2). Thus Y^{381} appears key to receptor activation, but is only directly involved in the binding of ACh and pilocarpine. This is supported by the ligand docking where 77-LH-28-1 is positioned some distance from Y^{381} (Figure 8), unlike dockings of ACh (Goodwin et al., 2007; Hulme et al., 2003).

At first sight, the role of F^{77} appears to be difficult to resolve based on the receptor model, as the residue faces away from the proposed ligand binding site (Figure 8). However, mutation of this residue has a clear effect to selectively reduce the efficacy of AC-42 and 77-LH-28-1 (Tables 2 and 3). On this basis we postulate that the aromatic side chain of F^{77} plays a role to stabilise the 'flipped out' gauche state of W^{101} *via* a π-π stacking interaction between the aromatic rings; this selectively enhances the function of AC-42 and 77-LH-28-1 whilst leaving pilocarpine and ACh unaffected. Therefore removal of the aromatic ring prevents this stabilisation and reduces the ability of 77-LH-28-1 to mediate receptor activation once bound.

Molecular Pharmacology Fast Forward. Published on April 22, 2010 as DOI: 10.1124/mol.110.064345
This article has not been copyedited and formatted. The final version may differ from this version.

Based on the data presented herein, AC-42 and 77-LH-28-1 may be better classed as bitopic, rather than allosteric, agonists, but definitive demonstration that such molecules contain both pure orthosteric and allosteric fragments is still required. Nonetheless, our mutational data have identified Y^{381} and W^{101} as selective differentiators of orthosteric versus novel agonist binding affinity, whilst revealing F^{77} as a novel and selective regulator of novel agonist efficacy. It will be interesting to see if additional functionally selective agonists that have been previously classed as "allosteric agonists" exhibit similar patterns of behavior.

Acknowledgments

The authors are grateful to Drs. Michael Crouch and Ron Osmond, TGR Biosciences, Adelaide, Australia, for the generous gift of *SureFire* ERK1/2 Kit reagents.

REFERENCES

Avlani VA, Gregory KJ, Morton CJ, Parker MW, Sexton PM and Christopoulos A (2007) Critical role for the second extracellular loop in the binding of both orthosteric and allosteric G protein-coupled receptor ligands. *J Biol Chem* **282**:25677-25686.

Ballesteros JA, Weinstein, H. (1995) Integrated methods for the construction of three-dimensional models and computational probing of structure-function relations in g protein-coupled receptors. *Meth Neurosci* **25**:366-428.

Birdsall NJM, Burgen ASV, Hulme EC, Stockton JM and Zigmond MJ (1983) The effect of McN-A-343 on muscarinic receptors in the cerebral cortex and heart. *Br J Pharmac* **78**:257-259.

Black JW and Leff P (1983) Operational models of pharmacological agonism. *Proc Roy Soc (Lond) B* **220**:141-162.

Blaney FE, Raveglia LF, Artico M, Cavagnera S, Dartois C, Farina C, Grugni M, Gagliardi S, Luttmann MA, Martinelli M, Nadler GM, Parini C, Petrillo P, Sarau HM, Scheideler MA, Hay DW and Giardina GA (2001) Stepwise modulation of neurokinin-3 and neurokinin-2 receptor affinity and selectivity in quinoline tachykinin receptor antagonists. *J Med Chem* **44**:1675-1689.

Bodick NC, Offen WW, Shannon HE, Satterwhite J, Lucas R, van Lier R and Paul SM (1997) The selective muscarinic agonist xanomeline improves both the cognitive deficits and behavioral symptoms of Alzheimer disease. *Alzh Dis Assoc Dis* **11**:S16-S22.

Bradford MM (1976) A rapid and sensitive method for the quantitation of microgram quantities of protein utilizing the principle of protein-dye binding. *Anal Biochem* **72**:248-254.

Cheng Y-C and Prusoff WH (1973) Relationship between the inhibition constant (K_I) and the concentration of inhibitor which causes 50 per cent inhibition (I_{50}) of an enzymatic reaction. *Biochem Pharmacol* **22**:3099-3108.

Cherezov V, Rosenbaum DM, Hanson MA, Rasmussen SG, Thian FS, Kobilka TS, Choi HJ, Kuhn P, Weis WI, Kobilka BK and Stevens RC (2007) High-resolution crystal structure of an engineered human beta2-adrenergic G protein-coupled receptor. *Science* **318**:1258-1265.

Christopoulos A (1998) Assessing the distribution of parameters in models of ligand-receptor interaction: to log or not to log. *Trends Pharmacol Sci* **19**:351-357.

Christopoulos A (2007) Muscarinic Acetylcholine Receptors in The Central Nervous System: Structure, Function and Pharmacology., in *Exploring The Vertebrate Central Cholinergic System* (Karczmar A ed) pp 163-208, Springer, New York.

Christopoulos A and Mitchelson F (1997) Pharmacological analysis of the mode of interaction of McN-A-343 at atrial muscarinic M_2 receptors. *Eur J Pharmacol* **339**:153-156.

Conn PJ, Christopoulos A and Lindsley CW (2009) Allosteric modulators of GPCRs: a novel approach for the treatment of CNS disorders. *Nature Rev Drug Discover* **8**:41-54.

Dunbrack RL, Jr. and Karplus M (1993) Backbone-dependent rotamer library for proteins. Application to side-chain prediction. *J Mol Biol* **230**:543-574.

Goodwin JA, Hulme EC, Langmead CJ and Tehan BG (2007) Roof and floor of the muscarinic binding pocket: variations in the binding modes of orthosteric ligands. *Mol Pharmacol* **72**:1484-1496.

Gregory KJ, Sexton PM and Christopoulos A (2007) Allosteric modulation of muscarinic acetylcholine receptors. *Curr Neuropharmacol* **5:** 157-167

Gregory KJ, Hall NE, Tobin AB, Sexton PM and Christopoulos A (2010) Identification of orthosteric and allosteric site mutations in M_2 muscarinic acetylcholine receptors that contribute to ligand-selective signaling bias. *J Biol Chem*. **285**:7459-7474.

Horton RM, Cai ZL, Ho SN and Pease LR (1990) Gene splicing by overlap extension: tailor-made genes using the polymerase chain reaction. *Biotechniques* **8**:528-535.

Hulme EC, Birdsall NJM and Buckley NJ (1990) Muscarinic receptor subtypes. *Ann Rev Pharmacol Toxicol* **30**:633-673.

Hulme EC, Lu ZL and Bee MS (2003) Scanning mutagenesis studies of the M_1 muscarinic acetylcholine receptor. *Recept Chann* **9**:215-228.

Jacobson MA, O'Brien JA, Pascarella D, Mallorga PJ, Scolnick EM and Sur C (2004) Mapping the interaction site of M_1 muscarinic receptor allosteric agonists. *Soc Neurosci Abstracts*.

Jones CK, Brady AE, Davis AA, Xiang Z, Bubser M, Tantawy MN, Kane AS, Bridges TM, Kennedy JP, Bradley SR, Peterson TE, Ansari MS, Baldwin RM, Kessler RM, Deutch AY, Lah JJ, Levey AI, Lindsley CW and Conn PJ (2008) Novel selective allosteric activator of the M1 muscarinic acetylcholine receptor regulates amyloid processing and produces antipsychotic-like activity in rats. *J Neurosci* **28**:10422-10433.

Kostenis E and Mohr K (1996) Two-point kinetic experiments to quantify allosteric effects on radioligand dissociation. *Trends Pharmacol Sci* **17**:280-283.

Langmead CJ, Austin NE, Branch CL, Brown JT, Buchanan KA, Davies CH, Forbes IT, Fry VA, Hagan JJ, Herdon HJ, Jones GA, Jeggo R, Kew JN, Mazzali A, Melarange R, Patel N, Pardoe J, Randall AD, Roberts C, Roopun A, Starr KR, Teriakidis A, Wood MD, Whittington M, Wu Z and Watson J (2008a) Characterization of a CNS penetrant, selective M_1 muscarinic receptor agonist, 77-LH-28-1. *Br J Pharmac* **154**:1104-1115.

Langmead CJ, Fry VA, Forbes IT, Branch CL, Christopoulos A, Wood MD and Herdon HJ (2006) Probing the molecular mechanism of interaction between 4-n-butyl-1-[4-(2-methylphenyl)-4-oxo-1-butyl]-piperidine (AC-42) and the muscarinic M(1) receptor: direct pharmacological evidence that AC-42 is an allosteric agonist. *Mol Pharmacol* **69**:236-246.

Langmead CJ, Watson J and Reavill C (2008b) Muscarinic acetylcholine receptors as CNS drug targets. *Pharm Ther* **117**:232-243.

Lazareno S and Birdsall NJM (1995) Detection, quantitation, and verification of allosteric interactions of agents with labeled and unlabeled ligands at G protein-coupled receptors: interactions of strychnine and acetylcholine at muscarinic receptors. *Mol Pharmacol* **48**:362-378.

Lebon G, Langmead CJ, Tehan BG and Hulme EC (2009) Mutagenic mapping suggests a novel binding mode for selective agonists of M_1 muscarinic acetylcholine receptors. *Mol Pharmacol* **75**:331-341.

Leff P, Dougall IG and Harper D (1993) Estimation of partial agonist affinity by interaction with a full agonist: a direct operational model-fitting approach. *Br J Pharmac* **110**:239-244.

Matsui H, Lazareno S and Birdsall NJ (1995) Probing of the location of the allosteric site on m1 muscarinic receptors by site-directed mutagenesis. *Mol Pharmacol* **47**:88-98.

May LT, Avlani VA, Langmead CJ, Herdon HJ, Wood MD, Sexton PM and Christopoulos A (2007) Structure-function studies of allosteric agonism at M2 muscarinic acetylcholine receptors. *Mol Pharmacol* **72**:463-476.

Motulsky HJ and Christopoulos A (2004) *Fitting models to biological data using linear and nonlinear regression. A practical guide to curve fitting.* Oxford University Press, New York.

Shekhar A, Potter WZ, Lightfoot J, Lienemann J, Dube S, Mallinckrodt C, Bymaster FP, McKinzie DL and Felder CC (2008) Selective muscarinic receptor agonist xanomeline as a novel treatment approach for schizophrenia. *Am J Psych* **165**:1033-1039.

Spalding TA, Ma JN, Ott TR, Friberg M, Bajpai A, Bradley SR, Davis RE, Brann MR and Burstein ES (2006) Structural requirements of transmembrane domain 3 for activation by the M1 muscarinic receptor agonists AC-42, AC-260584, clozapine, and N-desmethylclozapine: evidence for three distinct modes of receptor activation. *Mol Pharmacol* **70**:1974-1983.

Spalding TA, Trotter C, Skjaerbaek N, Messier TL, Currier EA, Burstein ES, Li D, Hacksell U and Brann MR (2002) Discovery of an ectopic activation site on the M(1) muscarinic receptor. *Mol Pharmacol* **61**:1297-1302.

Sur C, Mallorga PJ, Wittmann M, Jacobson MA, Pascarella D, Williams JB, Brandish PE, Pettibone DJ, Scolnick EM and Conn PJ (2003) N-desmethylclozapine, an allosteric agonist at muscarinic 1 receptor, potentiates N-methyl-D-aspartate receptor activity. *Proc Natl Acad Sci U S A* **100**:13674-13679.

Valant C, Gregory KJ, Hall NE, Scammells PJ, Lew MJ, Sexton PM and Christopoulos A (2008) A novel mechanism of G protein-coupled receptor functional selectivity. Muscarinic partial agonist McN-A-343 as a bitopic orthosteric/allosteric ligand. *J Biol Chem* **283**:29312-29321.

Valant C, Sexton PM and Christopoulos A (2009) Orthosteric/allosteric bitopic ligands: going hybrid at GPCRs. *Mol Interv* **9**:125-135.

Ward SD, Curtis CA and Hulme EC (1999) Alanine-scanning mutagenesis of transmembrane domain 6 of the M_1 muscarinic acetylcholine receptor suggests that Tyr381 plays key roles in receptor function. *Mol Pharmacol* **56**:1031-1041.

Wess J, Eglen RM and Gautam D (2007) Muscarinic acetylcholine receptors: mutant mice provide new insights for drug development. *Nature Rev Drug Discover* **6**:721-733.

Molecular Pharmacology Fast Forward. Published on April 22, 2010 as DOI: 10.1124/mol.110.064345
This article has not been copyedited and formatted. The final version may differ from this version.

FOOTNOTES

This work was funded by the National Health and Medical Research Council (NHMRC) of Australia [Program Grant No. 519461]. Arthur Christopoulos is a Senior, and Patrick Sexton a Principal, Research Fellow of the NHMRC.

1. Current address: School of Molecular and Microbial Biosciences, University of Sydney, Australia

2. Current address: Heptares Therapeutics, BioPark, Welwyn Garden City, Herts., U.K.

3. Current address: CNS Research, UCB S.A., Belgium.

Molecular Pharmacology Fast Forward. Published on April 22, 2010 as DOI: 10.1124/mol.110.064345
This article has not been copyedited and formatted. The final version may differ from this version.

LEGENDS FOR FIGURES

Figure 1. Structure of the novel agonists used in this study.

Figure 2. Comparison of equilibrium binding between 77-LH-28-1 and the prototypical allosteric mAChR modulator, C_7/3-phth. The interaction between each ligand and the orthosteric ligand, [^{3}H]NMS, was assessed at 37°C on membranes from CHO FlpIn cells stably expressing the human M_1 mAChR. The curves superimposed on the data points represent the best global nonlinear regression curve fit of an allosteric ternary complex model. Points represent the mean + standard error of the mean of 3 experiments performed in duplicate. Where error bars are not shown, they lie within the dimensions of the symbol.

Figure 3. 77-LH-28-1, recognizes part of the prototypical allosteric site on the [^{3}H]NMS-occupied M_1 mAChR. (**A**) [^{3}H]NMS dissociation determined in the absence or presence of C_7/3-phth or 77-LH-28-1 at 37°C on membranes from CHO FlpIn cells stably expressing the human M_1 mAChR. **(B**) Full concentration-response relationship of the effect of C_7/3-phth on the dissociation rate of [^{3}H]NMS at 37°C in the absence or presence of 77-LH-28-1. Data represent the mean + standard error of the mean obtained from three experiments conducted in duplicate. Where error bars are not shown, they lie within the dimensions of the symbol. Arrows indicate midpoint potency values.

Figure 4. Novel agonists have lower efficacy at the M_1 mAChR relative to ACh. (A) Effect of different expression levels of M_1 mAChR on ACh potency and maximal effect for mediating intracellular Ca^{++} elevation in U2OS cells transiently transduced using BacMam technology. **(B)** Comparison of orthosteric agonist- (ACh, pilocarpine) and novel agonist (77-LH-28-1, AC-42)-mediated intracellular Ca^{++} elevation in U2OS cells transiently transduced

Molecular Pharmacology Fast Forward. Published on April 22, 2010 as DOI: 10.1124/mol.110.064345
This article has not been copyedited and formatted. The final version may differ from this version.

with 2pfu/cell of M_1 mAChR. Points represent the mean + standard error of the mean of 3 experiments performed in duplicate. Where error bars are not shown, they lie within the dimensions of the symbol.

Figure 5. Functional interaction between ACh and 77-LH-28-1 is consistent with competition. Effect of increasing concentrations of **(A)** atropine or **(B)** 77-LH-28-1 on ACh-mediated intracellular Ca^{++} elevation in U2OS cells transiently transduced with 0.5 pfu/cell of M_1 mAChR. The curves superimposed on the data points represent the best global nonlinear regression curve fit of a competitive **(A)** Schild model or **(B)** operational model. Points represent the mean + standard error of the mean of 4-5 experiments performed in duplicate. Where error bars are not shown, they lie within the dimensions of the symbol.

Figure 6. Novel agonists display divergent sensitivity to key M_1 mAChR mutations relative to prototypical orthosteric agonists. Effect of increasing concentrations of agonist on M_1 on mAChR-mediated intracellular Ca^{++} elevation in U2OS cells transiently transduced with the indicated mutant M_1 mAChR. Points represent the mean + standard error of the mean of 3 experiments performed in duplicate.

Figure 7. Differential effect of M_1 mAChR $F^{77}I$ mutation on novel agonist efficacy is signaling pathway-independent. Effect of increasing concentrations of agonist on M_1 on mAChR-mediated phosphorylation of ERK1/2 in U2OS cells transiently transduced with the indicated mutant M_1 mAChR. Points represent the mean + standard error of the mean of 3 experiments performed in duplicate, and are normalized to the response mediated by 10% FBS. Where error bars are not shown, they lie within the dimensions of the symbol.

Molecular Pharmacology Fast Forward. Published on April 22, 2010 as DOI: 10.1124/mol.110.064345
This article has not been copyedited and formatted. The final version may differ from this version.

Figure 8. A proposed docking pose of 77-LH-28-1 is consistent with a bitopic mode at the M_1 mAChR. A molecular model showing two different views of the top of the TM bundle of the M_1 mAChR indicating an extended pose for 77-LH-28-1. The key residues mutated in the current study are also indicated.

Molecular Pharmacology Fast Forward. Published on April 22, 2010 as DOI: 10.1124/mol.110.064345
This article has not been copyedited and formatted. The final version may differ from this version.

Table 1 Ligand binding parameters for M_1 mAChR constructs derived from U2OS whole cell binding assays. Data represent the mean ± S.E.M. of 3 experiments performed in duplicate.

Ligand	**pK_A value [a]**			
	Wild Type	**$F^{77}I$**	**$W^{101}A$**	**$Y^{381}A$**
	(0.5 pfu/ml)	**(1.25 pfu/ml)**	**(0.5 pfu/ml)**	**(0.5 pfu/ml)**
[^{3}H]QNB	10.25 ± 0.12	10.69 ± 0.11	9.36 ± 0.03*	10.26 ± 0.02
Acetylcholine	4.46 ± 0.08	4.13 ± 0.11	3.33 ± 0.16*	2.39 ± 0.06*
Pilocarpine	5.10 ± 0.06	5.03 ± 0.06	4.59 ± 0.06*	3.56 ± 0.05*
AC-42	6.14 ± 0.04	6.04 ± 0.05	7.53 ± 0.08*	6.53 ± 0.04*
77-LH-28-1	6.74 ± 0.04	6.41 ± 0.04*	8.64 ± 0.06*	7.16 ± 0.04*
B_{max} [b]	13.85 ± 0.36	12.57 ± 1.70	23.73 ± 1.64*	15.78 ± 0.43*
(fmol/10^5 cells)	(1)	(0.91)	(1.71)	(1.14)

[a] Negative logarithm of the ligand equilibrium dissociation constant.

[b] Maximum density of binding sites. Parentheses indicate normalized expression levels relative to the wild type.

* Significantly different ($p < 0.05$) from the wild type receptor as determined by one-way ANOVA followed by Dunnett's post-test.

Molecular Pharmacology Fast Forward. Published on April 22, 2010 as DOI: 10.1124/mol.110.064345
This article has not been copyedited and formatted. The final version may differ from this version.

Table 2 Agonist coupling efficiency parameters for M_1 mAChR-mediated Ca^{++} elevation in U2OS cells. Data represent the mean ± S.E.M. of 4-8 experiments performed in duplicate.

Ligand	**Logτ_c value** [a]			
	Wild Type	**$F^{77}I$**	**$W^{101}A$**	**$Y^{381}A$**
	(0.5 pfu/ml)	**(1.25 pfu/ml)**	**(0.5 pfu/ml)**	**(0.5 pfu/ml)**
Acetylcholine	2.82 ± 0.07	2.83 ± 0.08	2.83 ± 0.07	2.23 ± 0.07*
	(661)	(676)	(676)	(169)
Pilocarpine	0.70 ± 0.06	0.44 ± 0.06	0.91 ± 0.07	-2.73 ± 0.94*
	(5)	(2.8)	(8.1)	(0.002)
AC-42	0.01 ± 0.05	-1.85 ± 0.58*	1.26 ± 0.06*	-0.77 ± 0.09
	(1)	(0.014)	(18.2)	(0.17)
77-LH-28-1	0.62 ± 0.06	-0.69 ± 0.11*	0.33 ± 0.06	-0.85 ± 0.10*
	(4.2)	(0.20)	(2.13)	(0.14)

[a] Logarithm of the relative coupling efficiency parameter, τ, was determined via nonlinear regression of the data to an operational model of agonism and corrected for receptor expression levels to yield a corrected τ_c parameter. Antilogarithm shown in parenthesis.

* Significantly different ($p < 0.05$) from the wild type receptor as determined by one-way ANOVA followed by Dunnett's post-test.

Molecular Pharmacology Fast Forward. Published on April 22, 2010 as DOI: 10.1124/mol.110.064345
This article has not been copyedited and formatted. The final version may differ from this version.

Table 3 Agonist coupling efficiency parameters for M_1 mAChR-mediated ERK1/2 phosphorylation in U2OS cells. Data represent the mean ± S.E.M. of 3 experiments performed in duplicate.

Ligand	Logτ_c value [a]	
	Wild Type (0.5 pfu/ml)	**$F^{77}I$ (1.25 pfu/ml)**
Acetylcholine	2.52 ± 0.03 (330)	2.57 ± 0.03 (371)
Pilocarpine	0.37 ± 0.03 (2.34)	0.29 ± 0.04 (1.94)
AC-42	0.00 ± 0.03 (1)	n.d.
77-LH-28-1	0.33 ± 0.03 (2.13)	-0.27 ± 0.03* (0.54)

[a] Logarithm of the relative coupling efficiency parameter, τ, was determined via nonlinear regression of the data to an operational model of agonism and corrected for receptor expression levels to yield a corrected τ_c parameter. Antilogarithm shown in parenthesis.

* Significantly different ($p < 0.05$) from the wild type receptor as determined by Student t-test.

Molecular Pharmacology Fast Forward. Published on April 22, 2010 as DOI: 10.1124/mol.110.064345
This article has not been copyedited and formatted. The final version may differ from this version.

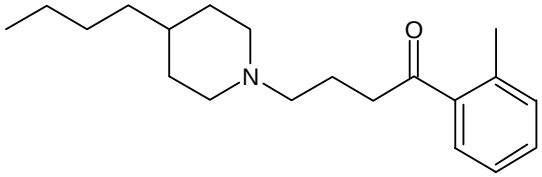

AC-42

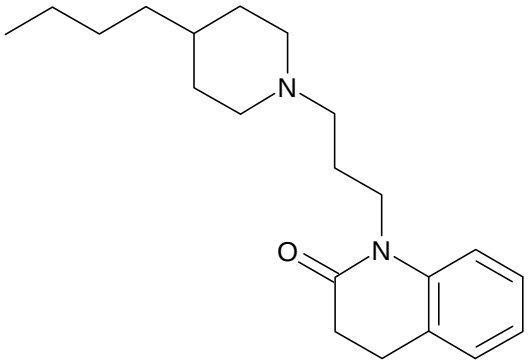

77-LH-28-1

Fig. 1

Molecular Pharmacology Fast Forward. Published on April 22, 2010 as DOI: 10.1124/mol.110.064345
This article has not been copyedited and formatted. The final version may differ from this version.

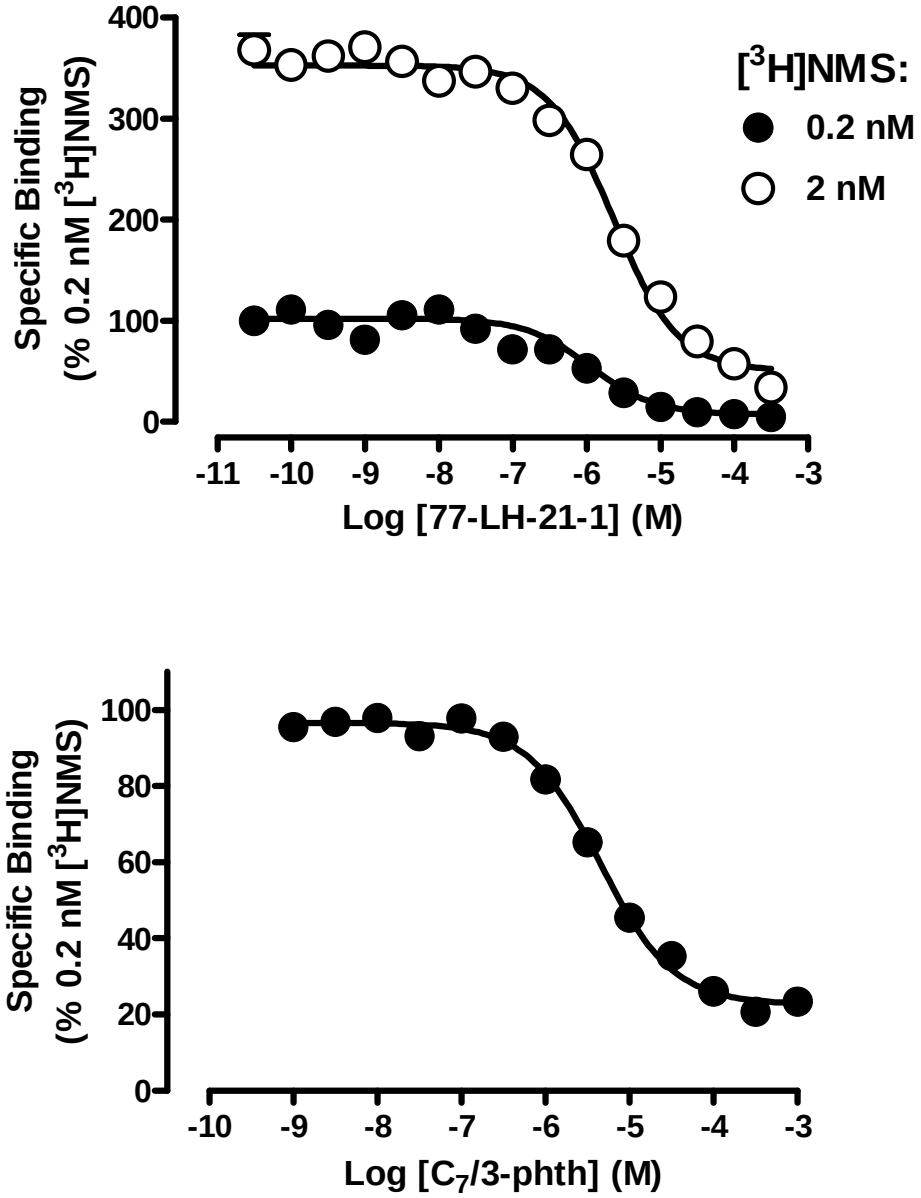

Fig. 2

Molecular Pharmacology Fast Forward. Published on April 22, 2010 as DOI: 10.1124/mol.110.064345
This article has not been copyedited and formatted. The final version may differ from this version.

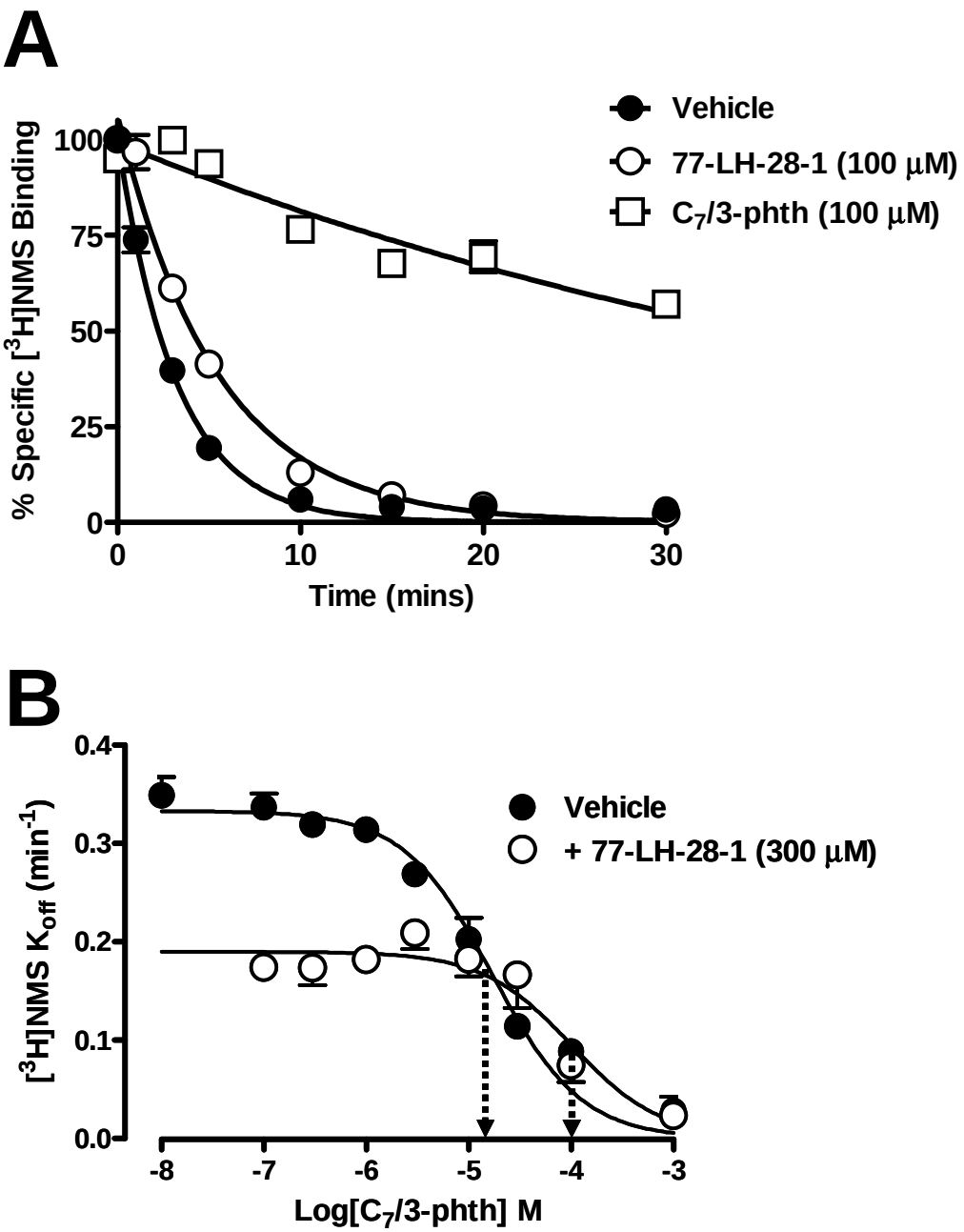

Fig. 3

Molecular Pharmacology Fast Forward. Published on April 22, 2010 as DOI: 10.1124/mol.110.064345
This article has not been copyedited and formatted. The final version may differ from this version.

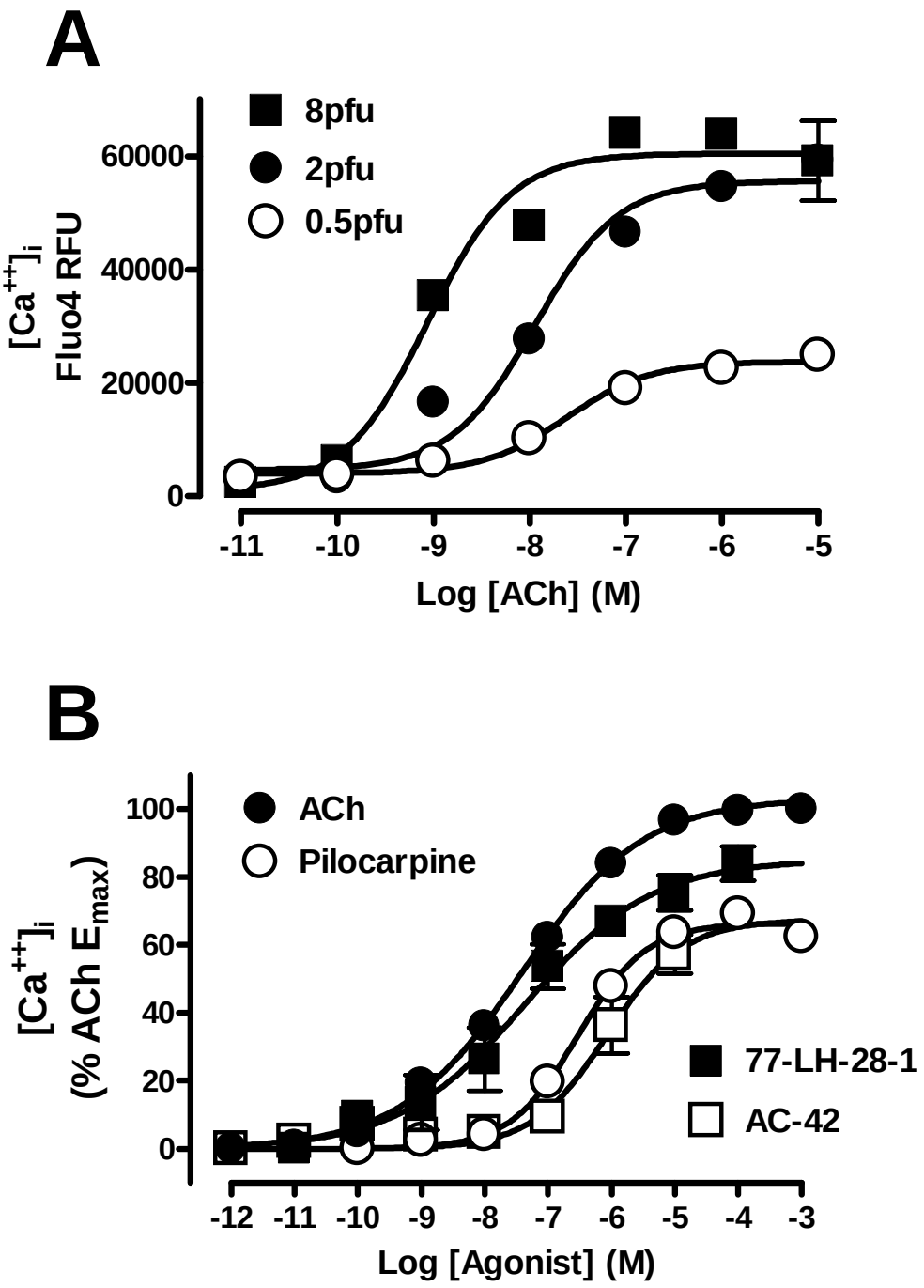

Fig. 4

Molecular Pharmacology Fast Forward. Published on April 22, 2010 as DOI: 10.1124/mol.110.064345
This article has not been copyedited and formatted. The final version may differ from this version.

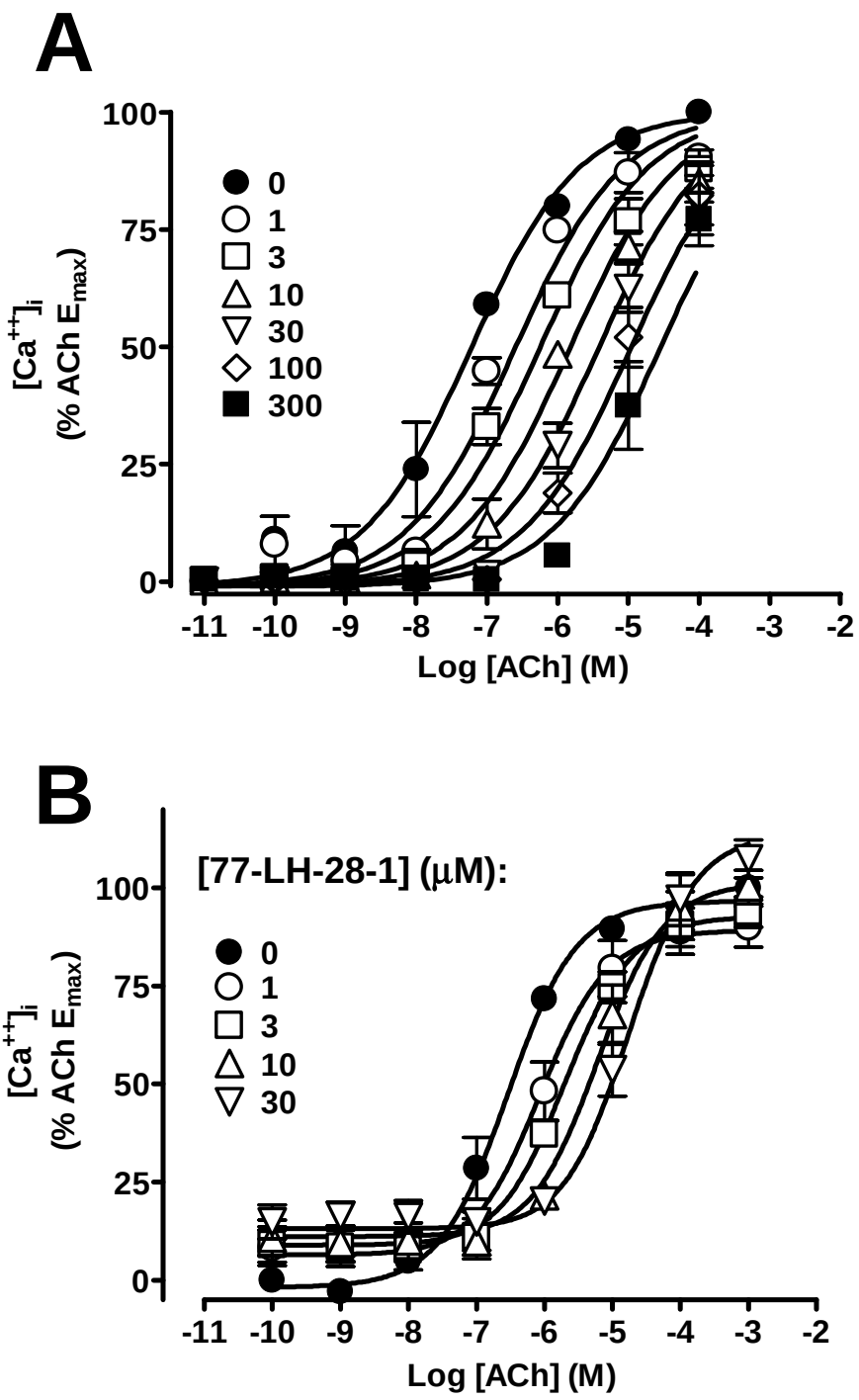

Fig. 5

Molecular Pharmacology Fast Forward. Published on April 22, 2010 as DOI: 10.1124/mol.110.064345
This article has not been copyedited and formatted. The final version may differ from this version.

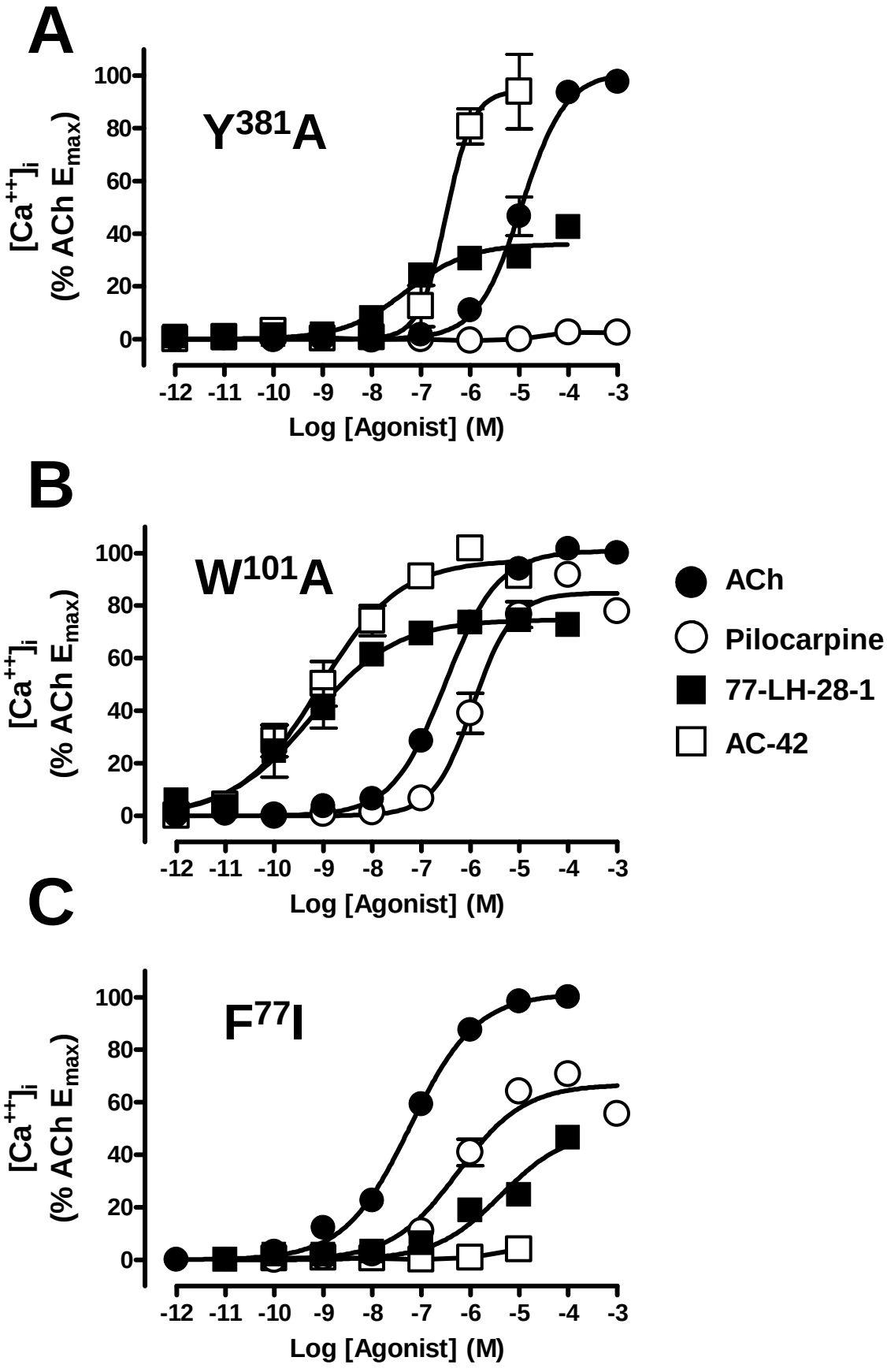

Fig. 6

Molecular Pharmacology Fast Forward. Published on April 22, 2010 as DOI: 10.1124/mol.110.064345
This article has not been copyedited and formatted. The final version may differ from this version.

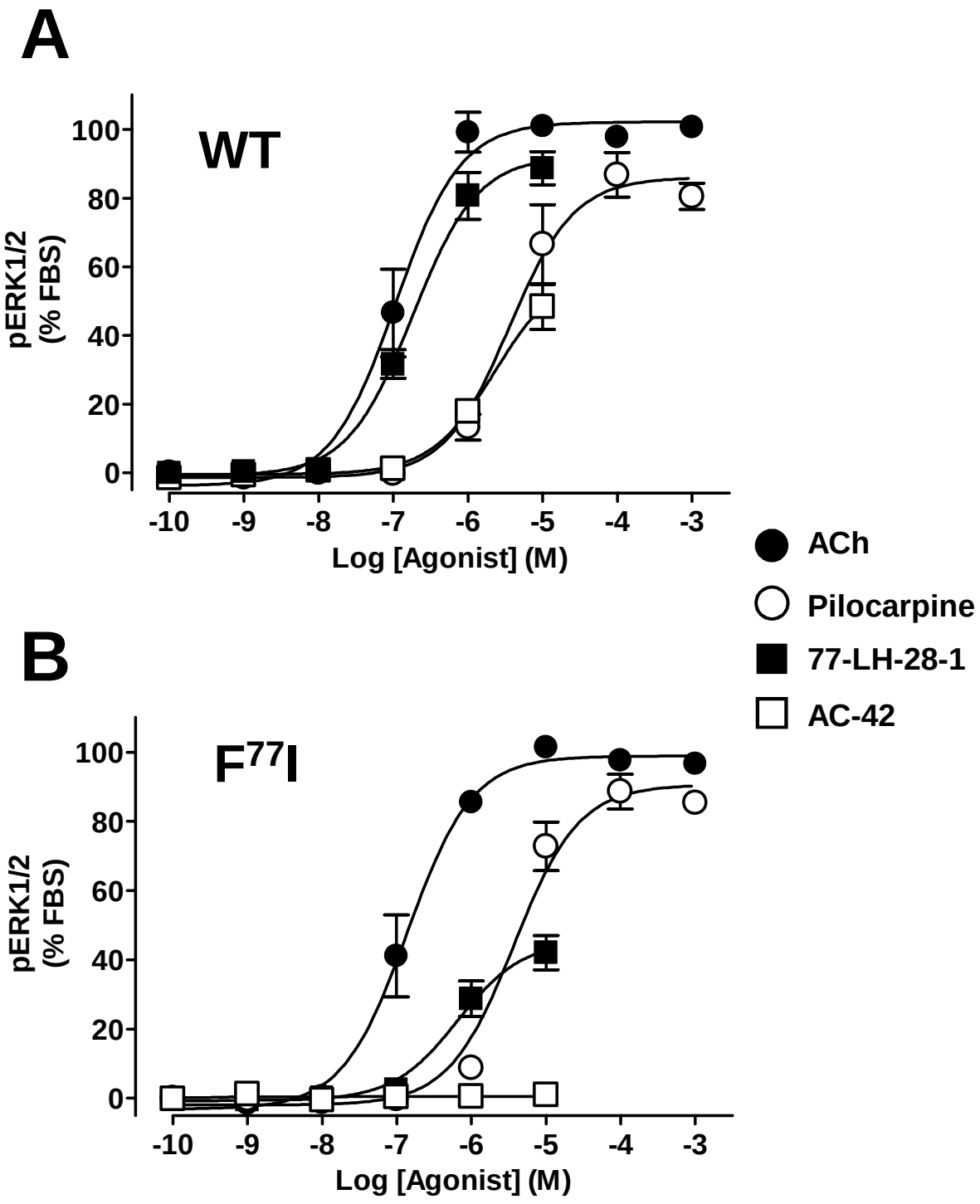

Fig. 7

Molecular Pharmacology Fast Forward. Published on April 22, 2010 as DOI: 10.1124/mol.110.064345
This article has not been copyedited and formatted. The final version may differ from this version.

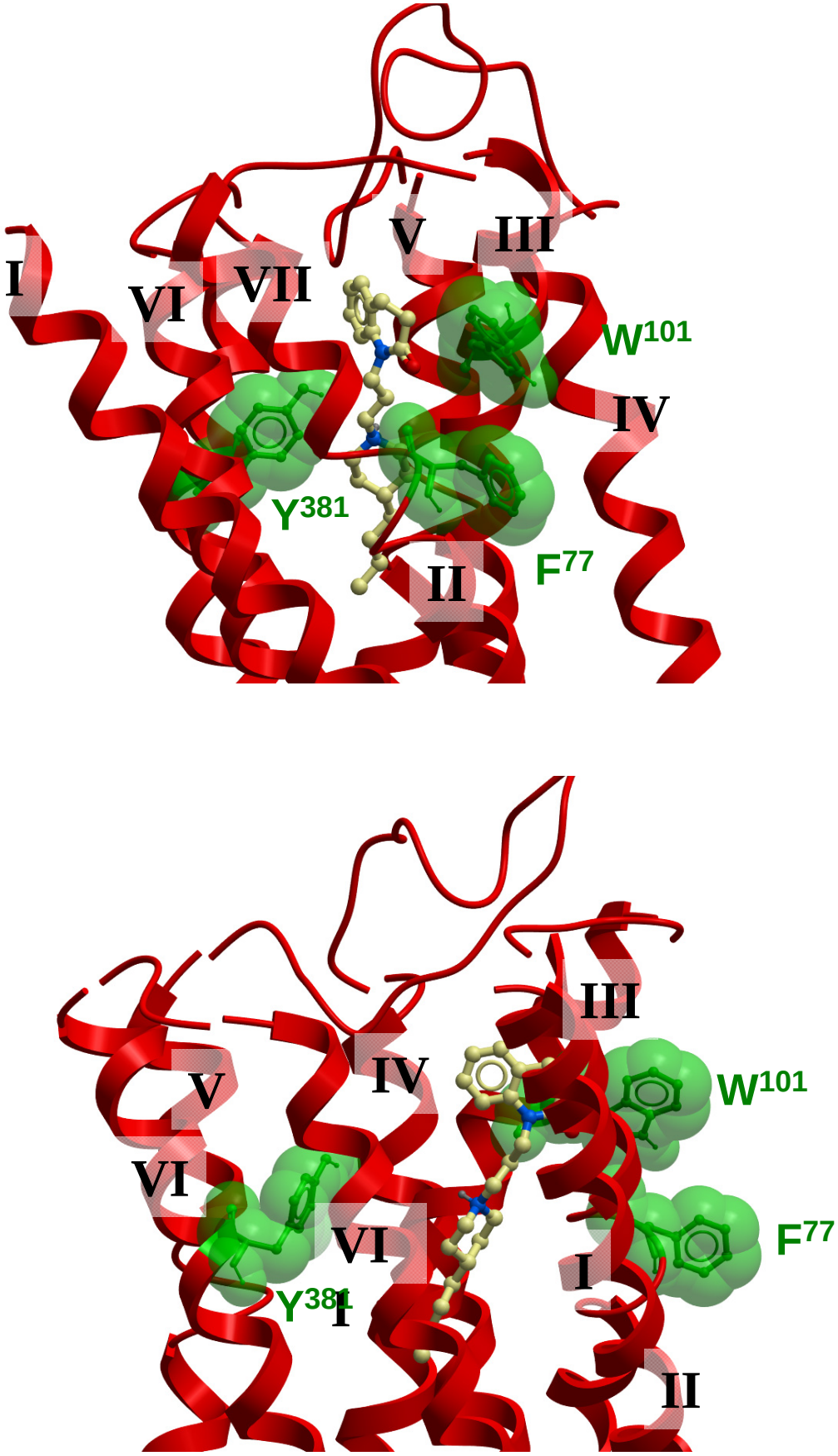

Fig. 8